

# Isotope Analysis Reveals Differential Impacts of Artificial and Natural Afforestation On Soil Organic Carbon Dynamics in Abandoned Farmland

Dongrui Di (✉ [didongrui@163.com](mailto:didongrui@163.com))

Sophia University: Jochi Daigaku

Guangwei Huang

Sophia University

---

## Research Article

**Keywords:** soil carbon stock, vegetation restoration, soil aggregate, soil respiration,  $^{13}\text{C}$ ,  $^{14}\text{C}$

**Posted Date:** October 1st, 2021

**DOI:** <https://doi.org/10.21203/rs.3.rs-238894/v2>

**License:**  This work is licensed under a Creative Commons Attribution 4.0 International License.

[Read Full License](#)

---

**Version of Record:** A version of this preprint was published at Plant and Soil on November 26th, 2021.  
See the published version at <https://doi.org/10.1007/s11104-021-05243-x>.

1 **Title:** Isotope analysis reveals differential impacts of artificial and natural  
2 afforestation on soil organic carbon dynamics in abandoned farmland

3

4 **Authors and Affiliations:**

5 Dong-Rui Di, Guang-Wei Huang\*

6 Graduate School of Global Environmental Studies, Sophia University, Tokyo  
7 102-8554, Japan

8

9 Dong-Rui Di

10 [didongrui@163.com](mailto:didongrui@163.com)

11

12 Guang-Wei Huang

13 [huanggwx@sophia.ac.jp](mailto:huanggwx@sophia.ac.jp)

14 **\*Corresponding authors:** Guang-Wei Huang, [huanggwx@sophia.ac.jp](mailto:huanggwx@sophia.ac.jp)

15 Tel/FAX: + 81-3-32384667

16

17 **Abstract:**

18 *Backgrounds* A multitude of studies have applied different methods to study the  
19 dynamics of soil organic carbon (SOC), but the differential impact of artificial and  
20 natural afforestation on SOC dynamic are still poorly understood.

21 *Methods and aims* We investigated the SOC dynamics following artificial and  
22 natural afforestation in Loess Plateau of China, characterizing soil structure and

23 stoichiometry using stable isotope carbon and radiocarbon models. We aim to  
24 compare SOC dynamics, clarify SOC source under different afforestation, examine  
25 comparability of the study areas and find how soil aggregate size classes control SOC  
26 dynamics, finally to evaluate effect of reforestation project.

27 *Results* The 0-10cm and 10-20 cm SOC stocks were significant higher than other  
28 two land-use system. At other depths, there is no significant difference among the  
29 three land-use system. Total top soil SOC stocks, C:N and C:P of differently sized soil  
30 aggregates significantly increased following afforestation.  $^{13}\text{C}$  results and  
31 Radiocarbon models indicated that the SOC decomposition rate and new SOC input  
32 rate were lower under natural afforestation than artificial afforestation.

33 *Conclusions* Afforestation can accumulate SOC in top soils mainly resulting  
34 from in topsoil changing. SOC resource is mainly from macroaggregate formation  
35 provided by fresh plant residues. SOC loss from soil respiration was derived from  
36 microaggregates during afforestation. The“space-for-time substitution” method is  
37 suitable for comparability of the study areas.

38

39 **Keywords:** soil carbon stock; vegetation restoration; soil aggregate; soil respiration;

40  $^{13}\text{C}$ ;  $^{14}\text{C}$

41

42

43

## 44 1. Introduction

45 Soil contains vast and dynamic pools of organic carbon that are fundamental for  
46 maintaining the balance of atmospheric CO<sub>2</sub> concentrations (Lal 2004; Post et al.  
47 1982).The soil organic carbon (SOC) pool and its dynamics are important properties  
48 of ecosystems (Schmidt et al. 2011). A multitude of studies report ecosystem changes  
49 significantly affect SOC pool and decomposition rate (Deng et al. 2016; Don et al.  
50 2011; Snell et al. 2015; Wei et al. 2013; Zhang et al. 2015).

51 The Loess Plateau is the one of the largest geographic units in China. Rapid  
52 population growth combining with climate and environmental conditions in the area  
53 have resulted in severe soil erosion in the Loess Plateau (Shi et al. 2017). Since 1950s,  
54 great attention has been paid to control the severe soil erosion in the Loess Plateau.  
55 From 1950s to mid-1960s, the principle soil conservation strategies were terracing on  
56 cultivated slopes and planting trees on uncultivated slopes. During the mid-1960s and  
57 the late 1970s, warp land dam and terracing became the most popular soil  
58 conservation strategies. From late 1970s to late 1990s, terracing became the first  
59 principle soil conservation strategy and natural rehabilitation appeared in some places  
60 (Zhou et al. 2013). The Grain for Green project was implemented in 1999 to halt soil  
61 erosion and promote ecological restoration in the region. As part of this project, both  
62 natural and artificial afforestation have been promoted as methods of ecological  
63 restoration (Shi et al. 2011).

64 Human ecosystem interventions such as deforestation and afforestation, can  
65 cause rapid and persistent changes in vegetation and soil. Wei et al. (2013) found SOC

66 stocks decreased most rapidly during the first 4 years of cropland cultivation after  
67 deforesting, but Rytter (2016) reported that SOC pools were generally unchanged  
68 after five years of *Salicaceae* growth during afforestation of former agricultural land.  
69 Natural change refers to the dynamic nature of ecosystem succession. Studies indicate  
70 that natural regeneration is slow and patchy with low species diversity (Blackham et  
71 al. 2014), and factors controlling SOC accumulation differed along vegetation  
72 succession (Liu et al. 2015).

73 Previous studies have applied different methods (e.g. space-for-time substitution,  
74 stable isotope analysis) to study SOC dynamics and have successfully answered  
75 questions related to soil structure and organic matter dynamics (Marin-Spiotta et al.  
76 2009; Qiu et al. 2015). However, these previous studies mainly focused on natural  
77 ecosystem restoration, without considering the effects of artificial restoration.  
78 Furthermore, although Deng et al. (2016) have investigated the SOC turnover during  
79 natural succession, SOC dynamics in stable post-succession communities (climax  
80 community) following afforestation remain unstudied.

81 In this study, we combined (1) a time dependent steady-state box model based on  
82 radiocarbon ( $^{14}\text{C}$ ) to estimate SOC decomposition rates in different land-use systems;  
83 (2) a natural abundance stable carbon isotope ( $^{13}\text{C}$ ) study to quantify old and new  
84 carbon turnover during both natural and artificial afforestation; (3) measures of  
85 change of SOC stock at different depth and soil aggregate-associated organic carbon  
86 (OC) & stoichiometry to investigate contribution of SOC change and the sensitivity  
87 and efficiency of soil aggregate-associated organic carbon with afforestation; and (4)

88 long-term field monitoring of soil respiration to assess SOC loss. We aim to compare  
89 SOC dynamics under both natural and artificial afforestation, clarify SOC source  
90 during afforestation period, examine comparability of the study areas and find how  
91 soil aggregate size classes control SOC dynamics, finally to evaluate effect of  
92 reforestation project.

## 93 **2. Materials and methods**

### 94 ***2.1. Study site***

95 The study site consisted of semi-arid forests located on Mt. Gonglushan, near Yan'an  
96 city in Shaanxi province, China (36°25.40"N, 109°31.53"E; 1245-1395m a.s.l.). On  
97 the Loess Plateau, precipitation and forest cover gradually decrease to the northwest,  
98 and our study site is located in the forest–grassland transition zone (Shi et al.  
99 2014). The 40-year averages (1971-2010) of annual precipitation and annual mean air  
100 temperature were 504.7 mm and 10.1 °C, respectively (Shi et al. 2012a). The soils are  
101 classified as Calcic Cambisols, which are derived from silt textured loess parent  
102 materials (Wei et al. 2013).

### 103 ***2.2. Field investigation and sampling***

104 We obtained estimates of the recovery periods of different communities from  
105 vegetation surveys from the 1950s to the early 2000s (Chen 1954; Fan et al. 2006;  
106 Zou et al. 2001) and records from local farmers and government (Tateno et al. 2007;  
107 Wang et al. 2010). These results have been accepted and used widely (Deng et al.  
108 2016; Qiu et al. 2015). The study examined two different types of afforestation:  
109 natural vegetation restoration from abandoned farmland to natural forest dominated

110 by *Quercus liaotungensis* Koidz (~80 years) (NQ) and artificial restoration from  
111 abandoned farmland to plantation dominated by *Robinia pseudoacacia* L. (~40 years)  
112 (AR). We compared these restoration types to a control site of abandoned farmland  
113 that remained unforested (AF). The three ecosystems were at least 3km apart. To  
114 minimize the effects of area conditions on experimental results, we selected study  
115 areas with similar topography, land-use history, and soil type. Five 20m×20m plots  
116 were established along the slope within each land use system for avoiding topographic  
117 influence: the upper position located on the top of the slope, the upper-middle position  
118 located between upper and middle positions, the middle position located on the  
119 middle of slope, the bottom-middle position located between bottom and middle  
120 positions and the bottom position located in the gully and adjacent area to the slope.  
121 Plots were spaced approximately 50m apart in each land-use system. Meanwhile, each  
122 plot was at least 40m from land-use system boundary to minimize edge effects.

123 We then dug five 20cm-deep pits for topsoil sampling at the four corners and the  
124 center in each plot, and took three soil bulk density (BD) samples. BD was measured  
125 at 0-20 cm in each subplot using a stainless steel cutting ring (5×5 cm). The soil cores  
126 were dried at 105°C for 24h. Five soil samples (0-20 cm) were collected from the five  
127 pits in each plot, and the collected samples were mixed to form one homogeneous  
128 sample for analysis of  $\delta^{13}\text{C}$ ,  $^{14}\text{C}$ , and aggregate size distribution. Three aggregate-size  
129 classes were manually fractionated through dry sieving of fresh soil samples on a  
130 series of two sieves (0.25 and 0.053mm) as follows: macroaggregates (>0.25mm),  
131 microaggregates (0.25-0.053mm) and silt & clay (<0.053mm). Fresh soil samples

132 were dry sieved because wet sieving compromised the *in situ* link between the  
133 aggregates obtained and their indigenous biota. Furthermore, wet sieving could cause  
134 inaccurate evaluation of soil organic carbon (Jiang et al. 2014). The subsamples of  
135 each aggregate fraction were used for soil organic carbon (SOC), total nitrogen (N),  
136 and total phosphorous (P) analysis. Each aggregate fraction was oven dried at 100°C  
137 and weighed to determine its proportion of total soil weight.

138         Meanwhile, SOC stock by investigation in deeper layers (0-1m) in June 2021.  
139         Totally, 45 soil profile were obtained for the investigation of 0-1m soil layers: 5pits/  
140         plot × 3 plots/ land-use system × 3 land-use system. Close to every topsoil sampling  
141         pits, the soil samples representing depths of 0–10 cm, 10–20 cm, 20–30 cm, 30–50 cm,  
142         50–100 cm were collected using a soil sampling auger (5-cm diameter) considering  
143         distribution of root systems (Shi et al. 2011; Tateno et al. 2007). The SOC, TN and  
144         bulk density of 0-1 m soil profiles were measured.

145         Additionally, the paired investigation site was set up in same land-use system  
146         with at least 3km distance between the paired sites ((NQ & paired NQ; AR & paired  
147         AR; AF & paired AF) for comparing soil characters of over 3km-distance sites in  
148         same land-use system in June 2021. The soil samples representing depths of 0–10 cm  
149         and 10–20 cm were collected using a soil sampling auger (5-cm diameter) for  
150         determining soil characters including soil organic carbon (SOC), total nitrogen (N),  
151         total phosphorous (P), fast potassium (K), pH and bulk density (BD).

### 152 **2.3. Laboratory analysis**

153         Soil organic carbon (SOC), total nitrogen (N), total phosphorous (P) and fast

154 potassium (K) were measured using a TOC VWP (Shimadzu, Japan), 2300 kjeltec  
155 analyzer unit (FOSS TECATOR, Sweden), and ICP-AES (Spectro, Analytical  
156 Instruments, Germany), respectively. Soil pH was determined using a soil/water ratio  
157 of 1:2.5 (PHSJ-4A pH acidometer, Shanghai, China). Soil organic carbon stock was  
158 calculated as the product of soil bulk density and SOC concentration.

159 Soil samples for  $\delta^{13}\text{C}$  analyses were pretreated with excess  $1\text{mol L}^{-1}\text{HCl}$  to  
160 remove carbonates at room temperature, then rinsed and freeze dried for at least 24 h  
161 and ground into fine powder over  $100\mu\text{m}$  meshes. Litters was washed with distilled  
162 water, then freeze-dried and ground into fine powder for measurement. The natural  
163 abundance of  $\delta^{13}\text{C}$  values in the soil organic matter and litter was analyzed with an  
164 Elemental Analyser (Eurovector) coupled to an isotope Ratio Mass Spectrometer  
165 (Delta plus, Thermo Fisher Scientific, USA) at the State key laboratory of Loess and  
166 Quaternary Geology at the Institute of Earth Environment, Chinese Academy of  
167 Sciences. Variation in the  $^{13}\text{C}/^{12}\text{C}$  was reported relative to the Vienna PDB standard,  
168 and is expressed as:

$$169 \quad \delta(\text{‰}) = \left( \frac{R_{\text{sample}}}{R_{\text{standard}}} - 1 \right) \times 1000 \quad (1)$$

170 Where  $R_{\text{sample}}$  is the  $^{13}\text{C}/^{12}\text{C}$  ratio of the sample and  $R_{\text{standard}}$  is the  $^{13}\text{C}/^{12}\text{C}$  ratio in  
171 the PDB standard.

172 The soil samples were pretreated for  $^{14}\text{C}$  analyses as standardized by Zhou et al.  
173 (1992). Measurement of  $^{14}\text{C}$  in soil organic matter was carried out at the Xi'an  
174 Accelerator Mass Spectrometry Center in the Institute of Earth Environment, Chinese  
175 Academy of Science. Cryogenically purified  $\text{CO}_2$  was converted to the target using

176 the hydrogen-iron reduction method. This method was described in detail by Zhu et al.  
177 (2010).

178

#### 179 **2.4. Measurement of soil respiration**

180 Soil respiration was measured using an automated soil CO<sub>2</sub> flux system (LI-8100,  
181 LI-COR, USA) equipped with a portable chamber (Model 8100-103). A PVC collar  
182 (20.3 cm in diameter and 10 cm in height) was inserted into the forest floor to a depth  
183 of 2.5 cm at each sampling point, approximately two months before the first  
184 measurements. Small litter and branches were left in the collar while large items were  
185 removed. All collars were left at the respective site for the entirety of the study period.

186 Soil respiration was measured over the 4-year period from 14 June 2010 to  
187 20 June 2014, approximately once every 30 days during April-October (growing  
188 season), and once every 45 days in other months (dormant season). The measurements  
189 were conducted between 8:30 and 11:30 local time on each sampling day. In each plot,  
190 five 5 m×5 m subplots were established at the four corners and the center. The PVC  
191 collars were installed in the center of each subplot for measurements of soil CO<sub>2</sub>  
192 efflux.

193

#### 194 **2.5. Data analysis**

195 Soil OC stocks were calculated as follow:

$$196 \text{ Soil OC stocks (kg m}^{-2}\text{)} = \frac{D \times BD \times OC}{100} \quad (2)$$

197 Where D is the thinness (cm) of the soil layer, BD is the bulk density (g cm<sup>-3</sup>), and

198 OC is the soil organic carbon concentrate ( $\text{g kg}^{-1}$ ) at 0-20 cm.

199 Stocks of soil OC in each soil aggregate size class were calculated as:

$$200 \text{ Stocks of } OC_i (\text{kg m}^{-2}) = \frac{D \times BD \times w_i \times OC_i}{10000} \quad (3)$$

201 Where  $OC_i$  is the soil organic carbon concentration of the  $i$ th aggregate size class ( $\text{g}$   
202  $\text{kg}^{-1}$  aggregate).

203 During the afforestation period, the decomposition rate constants  $k_1 (\text{yr}^{-1})$  was  
204 calculated by these models based on  $\delta^{13}\text{C}$  method: The proportions of new SOC ( $f_{\text{new}}$ )  
205 and old SOC ( $f_{\text{old}}$ ) were estimated based on the mass balance equations (Del Galdo et  
206 al. 2003):

$$207 f_{\text{new}} = \frac{(\delta_{\text{new}} - \delta_{\text{old}}) \times 100\%}{\delta_{\text{veg}} - \delta_{\text{old}}} \quad (4)$$

$$208 f_{\text{old}} = 100 - f_{\text{new}} \quad (5)$$

209 where  $\delta_{\text{new}}$  is the  $\delta^{13}\text{C}$  value of the soil sample from current ecosystem,  $\delta_{\text{old}}$  is the  $\delta^{13}\text{C}$   
210 value of the soil sample prior to ecosystem succession and  $\delta_{\text{veg}}$  is the  $\delta^{13}\text{C}$  value of the  
211 mixed litter of current vegetation. Decomposition rate constants ( $k_1$ ) of soil OC were  
212 estimated using the following equations (Marin-Spiotta et al. 2009):

$$213 k_1 = \frac{-\ln (C_t / C_0)}{t} \quad (6)$$

214 Where  $C_0$  is the initial SOC stock (SOC stock in the reference sites),  $C_t$  is initial SOC  
215 stock remaining (old C stock) at time  $t$  (year) since ecosystem change.

216 For the long-term ecosystem, the decomposition rate constants  $k_2 (\text{yr}^{-1})$  was  
217 obtained through the bomb- $^{14}\text{C}$  model (Cherkinsky and Brovkin 1993; Torn et al.  
218 2002; Trumbore 1993). The procedures were as follows (Tan et al. 2013):

219  $^{14}\text{C}$  data (pMC) is defined as

$$220 \quad \text{pMC}(\%) = \frac{A_{\text{SN}}}{A_{\text{ON}} \times e^{\lambda(y-1950)}} \times 100 \quad (7)$$

221 where  $A_{\text{SN}}$  is the  $^{14}\text{C}/^{12}\text{C}$  ratio of the sample corrected to a  $\delta^{13}\text{C}$  value of  $-25\%$  to  
222 account for the assumption that plants discriminate twice as much against  $^{14}\text{C}$  as they  
223 do against  $^{13}\text{C}$ ,  $A_{\text{ON}}$  is the  $^{14}\text{C}/^{12}\text{C}$  ratio of the oxalic acid activity normalized to  $\delta^{13}\text{C}$   
224 value of  $-19\%$ ,  $\lambda = 1/8267$  is based on the 5730 a half-life, and (y) is the year of  
225 Oxalic measurement.

226 The SOC turnover times were estimated using a time dependent steady-state box  
227 model. This assumes that variation in  $^{14}\text{C}$  in a soil with time follows a first-order  
228 kinetic law, which can be described by mass balance equation:

$$229 \quad C_y \times ^{14}C_y = C_{y-1} \times ^{14}C_{y-1} \times (1 - k_2 - \lambda) + I \times ^{14}C_{\text{atm},y-\text{lag}} \quad (8)$$

230 where  $C$  is the organic carbon inventory of a soil sample ( $\text{g C m}^{-2}$ ),  $^{14}C$  is the pMC of  
231 a soil sample (%),  $k$  is the first order decomposition constant for homogeneous C  
232 pools ( $\text{a}^{-1}$ ),  $\lambda$  is the  $^{14}\text{C}$  decay constant (1/8267),  $I$  is the annual carbon input ( $\text{g C m}^{-2}$   
233  $\text{a}^{-1}$ ),  $^{14}C_{\text{atm}}$  is the pMC of the atmosphere  $\text{CO}_2$  (%), lag is the average number of years  
234 that atmospheric  $\text{CO}_2$  is retained in plant tissue before becoming part of the soil  
235 organic matter pool. At steady state,  $C_y = C_{y-1}$  and  $I = kC$ , eq. (7) can be transformed  
236 into:

$$237 \quad ^{14}C_y = ^{14}C_{\text{atm},y-\text{lag}} \times k_2 + ^{14}C_{y-1} \times (1 - k_2 - \lambda) \quad (9)$$

238 The decomposition rate constant  $k_2$  is obtained by matching the modeled and  
239 measured pMC for the year in which the soil was sampled based on  $^{14}C_{\text{atm}}$  adopt from  
240 curve of  $^{14}\text{C}$  of atmospheric  $\text{CO}_2$ .

241 A method was proposed by Qiu et al. (2012) for assessing the relative  
242 contribution of changes in aggregate amount and aggregate-associated OC  
243 concentrations to the total changes in OC stocks within each aggregate fraction. It was  
244 assumed that changes in OC stock within any particular aggregate fraction were  
245 caused both by changes in OC concentration in the fraction ( $F_1$ ) and by changes in the  
246 mass of the fraction ( $F_2$ ). It was also assumed that the mass that was gained or lost  
247 from an aggregate fraction due to ecosystem change had the same OC concentration  
248 as the rest of that fraction after ecosystem change. We therefore calculated the  
249 contribution of  $F_1$  and  $F_2$  to the total change in OC stock within an aggregate fraction  
250 as follows:

$$251 \quad F_1 = M \times \Delta C \quad (11)$$

$$252 \quad F_2 = \Delta M \times C \quad (12)$$

253 where  $F_1$  is the change in OC stock ( $\text{g m}^{-2}$ ) within an aggregate fraction due to  
254 changes in aggregate-associated OC concentrations,  $F_2$  is the change in the OC stock  
255 ( $\text{gm}^{-2}$ ) within an aggregate fraction due to changes in the mass of the aggregate  
256 fraction,  $\Delta M$  is the change in the mass of a particular fraction ( $\text{kg m}^{-2}$ ),  $M$  is the initial  
257 mass of the aggregate fraction ( $\text{kg m}^{-2}$ ) before ecosystem change,  $C$  is the final OC  
258 concentration of the aggregate fraction ( $\text{g kg}^{-1}$ ) after ecosystem change and  $\Delta C$  is the  
259 change in the OC concentration of the aggregate fraction ( $\text{g kg}^{-1}$ ) due to ecosystem  
260 change.

## 261 ***2.6. Calculation of Annual soil CO<sub>2</sub> emissions***

262 Annual soil CO<sub>2</sub> emissions were estimated by interpolating the average CO<sub>2</sub> flux

263 rate between sampling dates, and computing the sum of the products of the average  
264 flux rate and the time between respective sampling dates for each measurement  
265 period(Shi et al. 2014; Shi et al. 2012b; Sims and Bradford 2001)as follows:

$$266 \quad R = \sum F_{m,n} \Delta t_n \quad (13)$$

267 Where  $\Delta t_n = t_{n+1} - t_n$ , which is the number of days between each field measurement  
268 within the year;  $R$  is total soil CO<sub>2</sub> emitted in the measurement period, and  $F_{m,n}$  is the  
269 average CO<sub>2</sub> flux rate over the interval  $t_{n+1} - t_n$  recorded by the LI-8100 Soil CO<sub>2</sub> Flux  
270 System.

## 271 **2.7 Statistical analyses**

272 One-way Analysis of Variation (ANOVA) with Pearson's test was performed to  
273 examine the difference between period of artificial and natural afforestation in topsoil  
274 SOC decomposition rate constants ( $k_1$ ) and new SOC input rate calculated with a <sup>13</sup>C  
275 model, and difference of contribution of  $F_1$  and  $F_2$  to the total change in SOC stock  
276 within an aggregate fraction between artificial and natural afforestation. Repeated  
277 measures ANOVA (RMANOVA) was applied to test the significance of SOC stocks at  
278 different soil depth, SOC in different soil aggregate size classes, soil aggregate size  
279 class distributions, C:N and C:P of different soil aggregate size classes, mean annual  
280 soil CO<sub>2</sub> emission, SOC decomposition rate constants ( $k_2$ ) calculated with a <sup>14</sup>C  
281 model among the three land use systems using Tukeys's HSD test at  $p < 0.05$ . All  
282 differences were evaluated at the 5% significance level.

283

284

## 285 **3. Results**

### 286 **3.1. The SOC stocks and contents**

287 The Fig 1 showed the soil organic carbon (SOC) stock (a) and soil organic  
288 carbon contents at each depth of the three different land-use systems, AF: abandoned  
289 farmland; AR: artificial afforestation (plantation of *Robinia pseudoacacia* L); NQ:  
290 natural afforestation (natural forest - *Quercus liaotungensis* Koidz). The SOC stock  
291 and content in 0-10 cm soil significantly increased with both artificial afforestation  
292 dominated by plantation of *Robinia pseudoacacia* L (AR) and natural afforestation  
293 dominated by natural forest *Quercus liaotungensis* Koidz (NQ).

294 Nevertheless, SOC stocks in 0-10 cm soil for artificial afforestation was  
295 significant lower than for natural afforestation. And the SOC stock and content in  
296 10-20cm soil in NQ is significantly higher than other two land-use systems, but there  
297 are no significant differences between in AR and AF. At other depths, there are no  
298 significant differences among the three land-use system. The results indicated  
299 accumulation of 0-1m SOC was mainly from 0-20cm topsoil changes under  
300 afforestation and was consistent with previous studies (Guillaume et al. 2015;  
301 Hiltbrunner et al. 2013; Song et al. 2016) .

### 302 **3.2. Aggregates organic carbon (OC) stocks, size distribution and C:N & C:P**

303 Fig 2a shows the difference of different aggregate size organic carbon (OC)  
304 stocks in the three land-use systems. Under both artificial and natural afforestation,  
305 the OC stocks of macroaggregates and microaggregates significantly increased, but  
306 the OC stocks of silt & clay were nearly 0 (far lower than for any other fraction), and

307 could thus be considered a negligible part of total OC stocks. The OC stock of  
308 macroaggregates was significant higher than that of microaggregate in AR, but the  
309 OC stock of macroaggregate and microaggregate were nearly the same in NQ.  
310 Meanwhile, The OC stock of macroaggregate and microaggregate in NQ were  
311 respectively significant lower and higher than in AR (Fig. 2a).

312 Macroaggregates and microaggregates accounted for approximate 99 % of the  
313 dry soil weight in the abandoned farmland. Under both artificial and natural  
314 restoration, the amount of soil in macroaggregates significantly increased, and  
315 microaggregates significantly decreased. There are no significant differences on the  
316 proportion of different size aggregate between in NQ and AR (Fig 2b). Furthermore,  
317 for both types of restorations, the amount of soils in silt & clay was less than 1% and  
318 did not significantly change.

319 Both C:N and C:P of different aggregate classes significantly increased with both  
320 types of afforestation. Compared with other size aggregates, C:N and C:P of  
321 microaggregates become higher after afforestation. Additionally, C:N and C:P in NQ  
322 were significantly higher than AR, except for C:N ratio of macroaggregates in NQ  
323 comparing with AR (Fig 3).

### 324 **3.3. Turnover of SOC and soil CO<sub>2</sub> emissions**

325 Over the afforestation period, the SOC decomposition rate ( $k_1$ ), and new SOC  
326 input rate ( $k_2$ ) under artificial restoration were higher than natural restoration (Fig 4).  
327 For the three land-use systems, the SOC decomposition rate ( $k_2$ ) was highest  
328 ( $2.6 \times 10^{-3}$ ) in the natural forest ecosystem (*Quercus liaotungensis* Koidz). The  $k_2$  of

329 abandoned farmland and plantation (*Robinia pseudoacacia* L.) were similar (Fig 5).

330 The amount of soil CO<sub>2</sub> emissions across ecosystems was calculated from  
331 continuous measurements over 4 years. Both natural and artificial restoration  
332 significantly increased the amount of soil CO<sub>2</sub> emissions, and the increased of amount  
333 of soil CO<sub>2</sub> emissions was higher under natural restoration (NQ) than artificial  
334 restoration (AR) (Fig 6).

#### 335 ***3.4. Contribution of mass and OC content in different soil aggregate size***

336 The aggregate-model (F<sub>1</sub> & F<sub>2</sub>) results show that the changes in F<sub>1</sub> & F<sub>2</sub> under  
337 artificial and natural restoration were nearly the same, and F<sub>1</sub> and F<sub>2</sub> significantly  
338 increased and decreased respectively, for macroaggregate-OC after afforestation, but  
339 changes in F<sub>1</sub> & F<sub>2</sub> for macroaggregate-OC were more significant under natural  
340 afforestation (Fig 7 a, b). In addition, F<sub>1</sub> significantly increased and F<sub>2</sub> slightly  
341 decreased for microaggregate-OC (Fig 7 c, d). The aggregate-model (F<sub>1</sub> & F<sub>2</sub>) results  
342 indicated that increases in SOC stocks in macroaggregates and microaggregates under  
343 artificial and natural afforestation were mainly due to increases in SOC concentration  
344 rather than mass (Fig 7). The contribution of macroaggregate-OC concentration  
345 increases under natural afforestation was more significant than under artificial, but  
346 microaggregate-OC changes under natural and artificial afforestation were similar.  
347 Therefore, we concluded that macroaggregate-OC stock is the main contributing  
348 factor to changes in total OC stock.

349

350

351 **4. Discussion**

352 ***4.1 Afforestation evaluation for SOC accumulation***

353 Restoration effect is the most important for evaluating reforestation project.  
354 Actually this is very difficult to find primeval forest as undisturbed site for direct  
355 comparison, because in this region there is no primary forest due to more than  
356 2000-years agricultural activity and semiarid climate. Until now the oldest secondary  
357 forest is about 200 years which is located in semi-humid region of Loess Plateau (Qiu  
358 et al. 2015). In this study, our results not only compared with other reforestation  
359 projects but also compared with 200-years secondary forest as "control" undisturbed  
360 sites for evaluating SOC accumulation under afforestation.

361 Laganière et al. (2010) summarize afforestation project data for investigating the  
362 influence of afforestation in agricultural soils on SOC stocks by 120 sites and 189  
363 observations globally. The study found that afforestation resulted in an increase in  
364 SOC stocks of 26% on average. In subtropical region, natural afforestation (secondary  
365 forest) and artificial afforestation in bare land increase ~190% and ~95% of 0-60 cm  
366 SOC stock respectively, but the afforestation still did not lead SOC stock to recover to  
367 level of undisturbed sites (primeval forest). The level of SOC stock in natural  
368 afforestation was only reach to ~60% of primeval forest (Wang et al. 2017). In  
369 sub-alpine region, afforestation in pasture resulted in 13 % increase of 0-80cm total  
370 SOC stocks, but the 60 % of increase was resulted from 0-10 cm topsoil (Hiltbrunner  
371 et al. 2013). Oppositely, the previous studies on deforestation as reference also can  
372 used to evaluate recovery of SOC stock after afforestation. Guillaume et al. (2018)

373 globally synthesize the impacts on SOC stock of rainforest conversion to tree  
374 plantations on carbon stocks and dynamics and found plantations lead to SOC stocks  
375 (0-50 cm) decreased by 10%-32%; van Straaten et al. (2015) indicated tropical  
376 deforestation for tree plantations decreased 0-300cm SOC stocks by up to 50%;  
377 Guillaume et al. (2015) showed SOC stocks (0-60 cm) decreased by 24%-42% under  
378 different plantations compared to the forest. The SOC stock reduction in plantations  
379 was significant down to topsoil (0-30 cm), but not when deeper layers were included.

380 In this study, natural afforestation (NQ) and artificial afforestation (AR) in  
381 abandoned farmland land increase 43% and 14% of total SOC stock (0-100 cm)  
382 respectively, and the 80 % of increase was resulted from 0-20 cm topsoil which was  
383 consistent with previous studies (Guillaume et al. 2015; Hiltbrunner et al. 2013).  
384 Comparing with 200-years secondary forest SOC stock (~33 Mg ha<sup>-1</sup> in 0-10 cm; ~16  
385 Mg ha<sup>-1</sup> in 10-20 cm) in semi-humid region of loess plateau (Qiu et al. 2015), natural  
386 afforestation in this study is reach up to the similar level. Additionally, our study also  
387 indicated SOC stocks (0-50 cm) in artificial afforestation (AR) was 30% lower than  
388 natural afforestation (NQ). This result also agrees with previous studies(Guillaume et  
389 al. 2015; van Straaten et al. 2015). In view of global afforestation projects or  
390 deforestation activities, we could conclude that afforestation in study area is effective  
391 for SOC accumulation, and natural afforestation is more significant than artificial.

392

#### 393 ***4.2 SOC source analysis based on aggregates and carbon isotope in topsoil***

394 A multitude of studies found that afforestation can lead to the accumulation of

395 SOC mainly resulting from increase of SOC in topsoil, and the effects of land use  
396 change during vegetation restoration on SOC are mainly due to changes in OC input  
397 and C mineralization (Deng et al. 2016; Laganière et al. 2010). The OC in soil  
398 physical fractions responds more sensitively and rapidly to land use change than the  
399 OC in bulk soils (Qiu et al. 2012; Wei et al. 2013); therefore, changes in  
400 aggregate-associated OC are regarded as fundamental processes for understanding the  
401 effects of vegetation restoration on SOC.

402 Stable isotope techniques provide an ideal tool for investigating the sources and  
403 dynamic of SOC based on the theory: the increase in proportion of new OC in soils  
404 could be attributed to the OC inputs from the new vegetation producing organic  
405 matter with different  $^{13}\text{C}/^{12}\text{C}$  ratio (Marin-Spiotta et al. 2009). And Richter et al.  
406 (1999) reported that the rates of new soil OC increase represented the net effect of  
407 new OC input including litterfall, rhizo-deposition and hydrological leaching of  
408 dissolved OC and output with organic matter mineralization to soils. Deng et al. (2016)  
409 summarize that sources of SOC resulting from vegetation restoration: (1) vegetation  
410 restoration facilitated SOC accumulation from biomass input (Tang et al. 2010).  
411 Vegetation biomass resulting from aboveground leaf litter and belowground roots is  
412 the main source of organic matter input into the soil (Laganière et al. 2010; Zhao et al.  
413 2015); (2) vegetation restoration probably contributed to the formation of stable soil  
414 aggregates (An et al. 2010), thus facilitating physical protection of SOC within  
415 aggregates (Lal 2004).

416 In our study, although it could be determined that new SOC resource is from  
417 vegetation biomass resulting from aboveground leaf litter and belowground roots due  
418 to afforestation in no-plant abandoned farmland, but our  $^{13}\text{C}$  result indicated old C  
419 decomposition and new C inputs during natural afforestation were significantly lower  
420 than during artificial afforestation (Fig 4); Meanwhile, the period of natural  
421 afforestation (~80 years) was twice as long as the period of artificial afforestation  
422 (~40 years). Though the new SOC input rate under natural afforestation was lower  
423 compared to artificial afforestation, the decomposition rate under natural afforestation  
424 was also lower, which may indicate higher SOC accumulation under natural  
425 afforestation is not attributable only to higher net increases in the difference between  
426 new SOC input and old SOC decomposition.

427 Besides, aggregate hierarchy theory points out that macro-aggregates contained  
428 less decomposed organic material, and had faster soil C turnover compared to  
429 micro-aggregates (Tisdall and Oades 1982). Some studies using  $^{13}\text{C}$  technology also  
430 confirm the theory and found the  $^{13}\text{C}$  in aggregates is enriched with decreasing  
431 aggregate size class in forest and farmland soils and SOC in macro-aggregates is  
432 younger and more labile than SOC in micro-aggregates (Liu et al. 2018a). That is  
433 because that lower  $\delta^{13}\text{C}$  values have been linked to more recent litter inputs, while  
434 higher  $\delta^{13}\text{C}$  values were related to older organic matter (Deng et al. 2016). All the  
435 previous studies concluded that fresh plant residues are the main agent for  
436 macroaggregate formation (Six and Paustian 2014).

437 In our study, the aggregate-model ( $F_1$  &  $F_2$ ) results indicated that increases in

438 SOC stocks were mainly due to increases in SOC concentration rather than mass in  
439 macroaggregates and microaggregates (Fig 7), and could conclude that  
440 macroaggregate-OC stock is the main contributing factor to changes in total SOC  
441 stock. Previous studies obtained a similar results (Liu et al. 2018b; Qiu et al. 2015).  
442 Combining with our and previous results, the studies confirms that SOC resource is  
443 mainly from macroaggregate formation provided by fresh plant residues. These results  
444 are also in accordance with previous observations

#### 445 ***4.3 SOC turnover and soil CO<sub>2</sub> emission***

446 time since land use change has not been considered as a key parameter for the  
447 accumulation of SOC. In this study, the period of natural afforestation was twice as  
448 long as the period of artificial afforestation. Though the new SOC input rate under  
449 natural afforestation was lower compared to artificial afforestation, the decomposition  
450 rate under natural afforestation was also lower, which may indicate higher SOC  
451 accumulation under natural afforestation is not attributable only to higher net  
452 increases in the difference between new SOC input and old SOC decomposition. We  
453 could conclude that time since land use change is a more important factor determining  
454 the proportions of new and old OC in soil. Previous studies lend support to this  
455 hypothesis.

456 Not only climax forest but also other types of ecosystems in semiarid or arid  
457 region often maintain in stable stage for a long time (Fan et al. 2006) and the  
458 dynamics of SOC in the ecosystem could be considered as an ecosystem property  
459 (Schmidt et al. 2011). <sup>14</sup>C dating has been proven to be an ideal tool to study the

460 dynamics of SOC from decadal to millennial timescales, which provides a direct  
461 measure of the time elapsed since carbon in organic matter was fixed from the  
462 atmosphere (Trumbore 1993). In this study, the steady-state box model of  $^{14}\text{C}$  of SOC  
463 was applied to estimate the mean residence time (MRT) of SOC for the long-term  
464 ecosystem, providing a sensitive indicator to quantify the proportion of SOC derived  
465 from the atmosphere in recent years to centuries based on the rate of incorporation of  
466 the nuclear explosion before 1960s carbon tracer (Laskar et al. 2016; Torn et al. 2009).  
467 In our study, the result of the  $^{14}\text{C}$  model suggested that the carbon decomposition rate  
468 was the lowest in the plantation (*Robinia pseudoacacia* L.) ecosystem, and was the  
469 same as abandoned farmland. The carbon decomposition rate was highest in the  
470 natural forest ecosystem (*Quercus liaotungensis* Koidz) (Fig 5). The model provided a  
471 direct evidence that higher accumulation of SOC under natural afforestation can be  
472 attributed to its longer restoration period rather than more rapid carbon turnover under  
473 natural afforestation compared to artificial afforestation. Therefore, our study suggests  
474 that longer recovery time could be more important for SOC accumulation following  
475 afforestation than any particular method of afforestation.

476         Additionally, soil respiration was always regarded as a kind of main pathway of  
477 soil OC loss (Shi et al. 2011). In this study, the result indicated that long-term soil  
478  $\text{CO}_2$  emission during afforestation promoted SOC loss via soil respiration, especially  
479 for natural afforestation (Fig 6). Meanwhile, the analysis of soil stoichiometry in the  
480 study suggested that C/N and C/P ratios in microaggregates were consistently higher  
481 than in other fractions under afforestation (Fig 3). And Spohn and Chodak (2015)

482 found that microorganisms increase their respiration rate with an increase in soil C/P  
483 ratio and C concentration. Therefore, combining our results with previous studies, it  
484 was concluded that SOC loss from soil respiration was mainly originated from  
485 microaggregate resulting from higher C/P ratio after afforestation, supporting the  
486 previous inference in terms of relationship between ecological stoichiometry and soil  
487 respiration (Spohn and Chodak 2015).

#### 488 ***4.4 Comparability of the study areas***

489 The comparability of the study areas is the central question in this study.  
490 Previous studies in this area also demonstrate topography greatly influence soil  
491 characters due to the hilly-gully topography (Shi et al. 2017; Tateno et al. 2017;  
492 Zhang et al. 2013). The studies found that the SOC, TN and other characters were  
493 significantly different along the hill slope. Therefore, in this study five 20 m×20 m  
494 plots were established along the slope within each land use system for avoiding  
495 topographic influence (detailed description of method in 2.2. *Field investigation and*  
496 *sampling*).

497 Additionally, the study area located in semiarid Loess Plateau, and rainfed  
498 agricultural areas are mainly distributed in the study areas and agricultural lands in  
499 this area are mostly on slopes (An et al. 2014). A lot of studies and documents  
500 reported that the semiarid region is always regarded as an entirety by reforestation  
501 project due to the same agriculture model, soil type, geological and climate condition  
502 of this region (He et al. 2014; Yamamoto and Endo 2014; Yamanaka et al. 2014) , and  
503 which is resulted in same land-use history. Base on high-density forest resources

504 inventory data and field measurements, Cui et al. (2015) and Li et al. (2017) analyses  
505 the carbon stock distribution patterns of forest ecosystems in Shaanxi Province of  
506 China (this study area located in the center of the province) and found spatial  
507 heterogeneity of soil characters and forest structure is not significant under the same  
508 forest age and tree species in semiarid region.

509 For a direct evidence, an invagination on characterization of the soils in the areas  
510 was carried out. The paired investigation site was set up in same land-use system with  
511 at least 3-km distance between the paired sites for comparing soil characters of over  
512 3km-distance sites in same land-use system. The characterization of the soils was  
513 presented in table 1 including SOC, TN, TP, fast K, pH and BD. The results showed  
514 soil characters between paired sites such as NQ & paired NQ, AR & paired AR, and  
515 AF & paired AF were not significant different, and then indicated homogeneity of soil  
516 characters in this area. The found was agreed with previous observations

517 In this study area, some studies using “space-for-time substitution” method has  
518 been published. The table 2 summarize the related information. All the previous  
519 studies more focused on edge effects of ecological transitional zone and topographic  
520 influence without spatial heterogeneity due to the high homogeneity of soil under  
521 same vegetation in this area. Therefore, in published studies the distances among  
522 different vegetation/ land-use types was required a reasonable long distance such as at  
523 least 3km for minimizing edge effects of ecological transitional zone. Therefore, we  
524 could conclude that the method especially for ~3km distance among different  
525 land-use systems is suitable for comparability of the study areas.

526 **5. Conclusions**

527 In conclusion, afforestation in study area is effective for SOC accumulation, and  
528 natural afforestation is more significant than artificial, which is mainly resulting from  
529 in topsoil changing. Carbon isotope and soil aggregates models analyzed that SOC  
530 resource is mainly from macroaggregate formation provided by fresh plant residues.  
531 The SOC concentration of soil aggregates played a dominant role in determining the  
532 dynamics of SOC accumulation during afforestation period. Based on the analysis of  
533 soil aggregates, soil respiration, and aggregate stoichiometry, we concluded that SOC  
534 loss from soil respiration mainly originated from microaggregates during afforestation.  
535  $^{13}\text{C}$  and  $^{14}\text{C}$  models proved effective tools that showed that recovery time is a key  
536 factor determining the accumulation of SOC following afforestation. Especially, the  
537 study confirm that “space-for-time substitution” method is suitable for comparability  
538 of the study areas.

539

540 **Acknowledgements**

541 We would like to thank Dr. Julia Monk at Yale University for her assistance with  
542 English language and grammatical editing. We also extended sincerely thank the three  
543 reviewers and Editor Dr. Lucas Silva for their valuable & excellent comments and  
544 suggestions, respectively. This research has been supported by projects from  
545 Engineered Food Production for Sustainable Agriculture Systems, Grand-in Aid for  
546 Challenging Research (Pioneering, No.20K20358).

547

548 **References**

- 549 An P, Inoue T, Zheng M, Eneji AE, Inanaga S (2014) Agriculture on the Loess Plateau.  
550 In: A Tsunekawa, G Liu, N Yamanaka, S Du (eds) Restoration and  
551 Development of the Degraded Loess Plateau, China. Springer Japan, Tokyo.
- 552 An S, Mentler A, Mayer H, Blum WEH (2010) Soil aggregation, aggregate stability,  
553 organic carbon and nitrogen in different soil aggregate fractions under forest  
554 and shrub vegetation on the Loess Plateau, China. CATENA 81: 226-233. doi:  
555 <https://doi.org/10.1016/j.catena.2010.04.002>.
- 556 Blackham GV, Webb EL, Corlett RT (2014) Natural regeneration in a degraded  
557 tropical peatland, Central Kalimantan, Indonesia: Implications for forest  
558 restoration. Forest Ecol Manag 324: 8-15. doi:  
559 <http://dx.doi.org/10.1016/j.foreco.2014.03.041>.
- 560 Chen C (1954) The vegetation and its roles in soil and water conservation in the  
561 secondary forest area in the boundary of Shaanxi and Gansu provinces. Acta  
562 Phytocologica et Geobotanica Sinica (in Chinese)(2): 152-223.
- 563 Cherkinsky AE, Brovkin VA (1993) Dynamics of radiocarbon in soils. Radiocarbon  
564 35: 363-367.
- 565 Cui G, Chen Y, Cao Y, An C (2015) Analysis on carbon stock distribution patterns of  
566 forest ecosystems in Shaanxi Province. Chinese Journal of Plant Ecology 39:  
567 333-342.
- 568 Del Galdo I, Six J, Peressotti A, Francesca Cotrufo M (2003) Assessing the impact of  
569 land-use change on soil C sequestration in agricultural soils by means of

570 organic matter fractionation and stable C isotopes. *Global Change Biol* 9:  
571 1204-1213. doi: 10.1046/j.1365-2486.2003.00657.x.

572 Deng L, Wang K-B, Chen M-L, Shangguan Z-P, Sweeney S (2013) Soil organic  
573 carbon storage capacity positively related to forest succession on the Loess  
574 Plateau, China. *CATENA* 110: 1-7. doi:  
575 <https://doi.org/10.1016/j.catena.2013.06.016>.

576 Deng L, Wang K, Tang Z, Shangguan Z (2016) Soil organic carbon dynamics  
577 following natural vegetation restoration: Evidence from stable carbon isotopes  
578 ( $\delta^{13}C$ ). *Agriculture, Ecosyst Environ* 221: 235-244. doi:  
579 <http://dx.doi.org/10.1016/j.agee.2016.01.048>.

580 Don A, Schumacher J, Freibauer A (2011) Impact of tropical land-use change on soil  
581 organic carbon stocks - a meta-analysis. *Global Change Biol* 17: 1658-1670.  
582 doi: 10.1111/j.1365-2486.2010.02336.x.

583 Fan W-Y, Wang X-A, Guo H (2006) Analysis of plant community successional series  
584 in the Ziwuling area on the Loess Plateau. *Acta Ecologica Sinica* 26: 706-714.

585 Guillaume T, Damris M, Kuzyakov Y (2015) Losses of soil carbon by converting  
586 tropical forest to plantations: erosion and decomposition estimated by  $\delta^{13}C$ .  
587 *Global Change Biol* 21: 3548-3560. doi: <https://doi.org/10.1111/gcb.12907>.

588 Guillaume T, Kotowska MM, Hertel D, Knohl A, Krashevskaya V, Murtillaksono K,  
589 Scheu S, Kuzyakov Y (2018) Carbon costs and benefits of Indonesian  
590 rainforest conversion to plantations. *Nat Commun* 9: 2388. doi:  
591 10.1038/s41467-018-04755-y.

592 He J-F, Guan J-H, Zhang W-H (2014) Land Use Change and Deforestation on the  
593 Loess Plateau. In: A Tsunekawa, G Liu, N Yamanaka, S Du (eds) Restoration  
594 and Development of the Degraded Loess Plateau, China. Springer Japan,  
595 Tokyo.

596 Hiltbrunner D, Zimmermann S, Hagedorn F (2013) Afforestation with Norway spruce  
597 on a subalpine pasture alters carbon dynamics but only moderately affects soil  
598 carbon storage. *Biogeochemistry* 115: 251-266. doi:  
599 10.1007/s10533-013-9832-6.

600 Jiang Y, Jin C, Sun B (2014) Soil aggregate stratification of nematodes and ammonia  
601 oxidizers affects nitrification in an acid soil. *Environmental Microbiol* 16:  
602 3083-3094. doi: 10.1111/1462-2920.12339.

603 Laganière J, Angers DA, ParÉ D (2010) Carbon accumulation in agricultural soils  
604 after afforestation: a meta-analysis. *Global Change Biol* 16: 439-453. doi:  
605 10.1111/j.1365-2486.2009.01930.x.

606 Lal R (2004) Soil carbon sequestration impacts on global climate change and food  
607 security. *Science* 304: 1623-1627. doi: 10.1126/science.1097396.

608 Laskar AH, Yadava MG, Ramesh R (2016) Radiocarbon and Stable Carbon Isotopes  
609 in Two Soil Profiles from Northeast India. *Radiocarbon* 54: 81-89. doi:  
610 10.2458/azu\_js\_rc.v54i1.15840.

611 Li X, Wang F, Cao Y, Peng S, Chen Y (2017) Soil carbon storage and its determinants  
612 in the forests of Shaanxi Province, China. *Chinese Journal of Plant Ecology* 41:  
613 953-963.

- 614 Liu S, Zhang W, Wang K, Pan F, Yang S, Shu S (2015) Factors controlling  
615 accumulation of soil organic carbon along vegetation succession in a typical  
616 karst region in Southwest China. *Sci Total Environ* 521–522: 52-58. doi:  
617 <http://dx.doi.org/10.1016/j.scitotenv.2015.03.074>.
- 618 Liu Y, Hu C, Hu W, Wang L, Li Z, Pan J, Chen F (2018a) Stable isotope fractionation  
619 provides information on carbon dynamics in soil aggregates subjected to  
620 different long-term fertilization practices. *Soil Till Res* 177: 54-60. doi:  
621 <https://doi.org/10.1016/j.still.2017.11.016>.
- 622 Liu Y, Liu W, Wu L, Liu C, Wang L, Chen F, Li Z (2018b) Soil aggregate-associated  
623 organic carbon dynamics subjected to different types of land use: Evidence  
624 from <sup>13</sup>C natural abundance. *Ecol Eng* 122: 295-302. doi:  
625 <https://doi.org/10.1016/j.ecoleng.2018.08.018>.
- 626 Marin-Spiotta E, Silver WL, Swanston CW, Ostertag R (2009) Soil organic matter  
627 dynamics during 80 years of reforestation of tropical pastures. *Global Change*  
628 *Biol* 15: 1584-1597. doi: 10.1111/j.1365-2486.2008.01805.x.
- 629 Post WM, Emanuel WR, Zinke PJ, Stangenberger AG (1982) Soil carbon pools and  
630 world life zones. *Nature* 298: 156-159. doi: 10.1038/298156a0.
- 631 Qiu L, Wei X, Zhang X, Cheng J, Gale W, Guo C, Long T (2012) Soil organic carbon  
632 losses due to land use change in a semiarid grassland. *Plant Soil* 355: 299-309.  
633 doi: 10.1007/s11104-011-1099-x.
- 634 Qiu LP, Wei XR, Gao JL, Zhang XC (2015) Dynamics of soil aggregate-associated  
635 organic carbon along an afforestation chronosequence. *Plant Soil* 391:

636 237-251. doi: 10.1007/s11104-015-2415-7.

637 Richter DD, Markewitz D, Trumbore SE, Wells CG (1999) Rapid accumulation and  
638 turnover of soil carbon in a re-establishing forest. *Nature* 400: 56-58. doi:  
639 10.1038/21867.

640 Rytter RM (2016) Afforestation of former agricultural land with Salicaceae species -  
641 Initial effects on soil organic carbon, mineral nutrients, C:N and pH. *Forest*  
642 *Ecol Manag* 363: 21-30. doi: 10.1016/j.foreco.2015.12.026.

643 Schmidt MWI, Torn MS, Abiven S, Dittmar T, Guggenberger G, Janssens IA, Kleber  
644 M, Kogel-Knabner I, Lehmann J, Manning DAC, Nannipieri P, Rasse DP,  
645 Weiner S, Trumbore SE (2011) Persistence of soil organic matter as an  
646 ecosystem property. *Nature* 478: 49-56. doi: 10.1038/nature10386.

647 Shi WY, Du S, Morina JC, Guan JH, Wang KB, Ma MG, Yamanaka N, Tateno R  
648 (2017) Physical and biogeochemical controls on soil respiration along a  
649 topographical gradient in a semiarid forest. *Agr Forest Meteorol* 247: 1-11. doi:  
650 10.1016/j.agrformet.2017.07.006.

651 Shi WY, Tateno R, Zhang JG, Wang YL, Yamanaka N, Du S (2011) Response of soil  
652 respiration to precipitation during the dry season in two typical forest stands in  
653 the forest-grassland transition zone of the Loess Plateau. *Agr Forest Meteorol*  
654 151: 854-863. doi: 10.1016/j.agrformet.2011.02.003.

655 Shi WY, Yan MJ, Zhang JG, Guan JH, Du S (2014) Soil CO<sub>2</sub> emissions from five  
656 different types of land use on the semiarid Loess Plateau of China, with  
657 emphasis on the contribution of winter soil respiration. *Atmos Environ* 88:

658 74-82. doi: 10.1016/j.atmosenv.2014.01.066.

659 Shi WY, Zhang JG, Yan MJ, Yamanaka N, Du S (2012a) Seasonal and diurnal  
660 dynamics of soil respiration fluxes in two typical forests on the semiarid Loess  
661 Plateau of China: Temperature sensitivities of autotrophs and heterotrophs and  
662 analyses of integrated driving factors. *Soil Biol Biochem* 52: 99-107. doi:  
663 10.1016/j.soilbio.2012.04.020.

664 Shi XH, Zhang XP, Yang XM, Drury CF, McLaughlin NB, Liang AZ, Fan RQ, Jia SX  
665 (2012b) Contribution of winter soil respiration to annual soil CO<sub>2</sub> emission in  
666 a Mollisol under different tillage practices in northeast China (Vol 26, GB2007,  
667 doi: 2011GB004054). *Glob Biogeochem Cycle* 26: GB3020. doi:  
668 10.1029/2012gb004477.

669 Sims PL, Bradford JA (2001) Carbon dioxide fluxes in a southern plains prairie. *Agr*  
670 *Forest Meteorol* 109: 117-134. doi:  
671 [http://dx.doi.org/10.1016/S0168-1923\(01\)00264-7](http://dx.doi.org/10.1016/S0168-1923(01)00264-7).

672 Six J, Paustian K (2014) Aggregate-associated soil organic matter as an ecosystem  
673 property and a measurement tool. *Soil Biol Biochem* 68: A4-A9. doi:  
674 <https://doi.org/10.1016/j.soilbio.2013.06.014>.

675 Snell HSK, Robinson D, Midwood AJ (2015) Tree species' influences on soil carbon  
676 dynamics revealed with natural abundance <sup>13</sup>C techniques. *Plant Soil* 400:  
677 285-296. doi: 10.1007/s11104-015-2731-y.

678 Song B-L, Yan M-J, Hou H, Guan J-H, Shi W-Y, Li G-Q, Du S (2016) Distribution of  
679 soil carbon and nitrogen in two typical forests in the semiarid region of the

680 Loess Plateau, China. CATENA 143: 159-166. doi:  
681 <https://doi.org/10.1016/j.catena.2016.04.004>.

682 Spohn M, Chodak M (2015) Microbial respiration per unit biomass increases with  
683 carbon-to-nutrient ratios in forest soils. Soil Biol Biochem 81: 128-133. doi:  
684 <http://dx.doi.org/10.1016/j.soilbio.2014.11.008>.

685 Tan W, Zhou L, Liu K (2013) Soil aggregate fraction-based <sup>14</sup>C analysis and its  
686 application in the study of soil organic carbon turnover under forests of  
687 different ages. Chinese Sci Bull 58: 1936-1947. doi:  
688 [10.1007/s11434-012-5660-7](https://doi.org/10.1007/s11434-012-5660-7).

689 Tang X, Liu S, Liu J, Zhou G (2010) Effects of vegetation restoration and slope  
690 positions on soil aggregation and soil carbon accumulation on heavily eroded  
691 tropical land of Southern China. J Soil Sediment 10: 505-513. doi:  
692 [10.1007/s11368-009-0122-9](https://doi.org/10.1007/s11368-009-0122-9).

693 Tateno R, Taniguchi T, Zhang J, Shi W-Y, Zhang J-G, Du S, Yamanaka N (2017) Net  
694 primary production, nitrogen cycling, biomass allocation, and resource use  
695 efficiency along a topographical soil water and nitrogen gradient in a  
696 semi-arid forest near an arid boundary. Plant Soil 420: 209-222. doi:  
697 [10.1007/s11104-017-3390-y](https://doi.org/10.1007/s11104-017-3390-y).

698 Tateno R, Tokuchi N, Yamanaka N, Du S, Otsuki K, Shimamura T, Xue Z, Wang S,  
699 Hou Q (2007) Comparison of litterfall production and leaf litter decomposition  
700 between an exotic black locust plantation and an indigenous oak forest near  
701 Yan'an on the Loess Plateau, China. Forest Ecol Manag 241: 84-90. doi:

702 <http://dx.doi.org/10.1016/j.foreco.2006.12.026>.

703 Tisdall JM, Oades JM (1982) Organic matter and water-stable aggregates in soils. *J*  
704 *Soil Sci* 33: 141-163. doi: <https://doi.org/10.1111/j.1365-2389.1982.tb01755.x>.

705 Torn MS, Lapenis AG, Timofeev A, Fischer ML, Babikov BV, Harden JW (2002)  
706 Organic carbon and carbon isotopes in modern and 100-year-old-soil archives  
707 of the Russian steppe. *Global Change Biol* 8: 941-953. doi:  
708 [10.1046/j.1365-2486.2002.00477.x](https://doi.org/10.1046/j.1365-2486.2002.00477.x).

709 Torn MS, Swanston CW, Castanha C, Trumbore SE (2009) Storage and Turnover of  
710 Organic Matter in Soil. *Biophysico-Chemical Processes Involving Natural*  
711 *Nonliving Organic Matter in Environmental Systems*.

712 Trumbore SE (1993) Comparison of carbon dynamics in tropical and temperate soils  
713 using radiocarbon measurements. *Glob Biogeochem Cycle* 7: 275-290. doi:  
714 [10.1029/93gb00468](https://doi.org/10.1029/93gb00468).

715 van Straaten O, Corre MD, Wolf K, Tchienkoua M, Cuellar E, Matthews RB,  
716 Veldkamp E (2015) Conversion of lowland tropical forests to tree cash crop  
717 plantations loses up to one-half of stored soil organic carbon. *P Natl Acad Sci*  
718 *USA*: 201504628. doi: [10.1073/pnas.1504628112](https://doi.org/10.1073/pnas.1504628112).

719 Wang F, Ding Y, Sayer EJ, Li Q, Zou B, Mo Q, Li Y, Lu X, Tang J, Zhu W, Li Z (2017)  
720 Tropical forest restoration: Fast resilience of plant biomass contrasts with slow  
721 recovery of stable soil C stocks. *Funct Ecol* 31: 2344-2355. doi:  
722 <https://doi.org/10.1111/1365-2435.12925>.

723 Wang K, Shao R, Shanguan Z (2010) Changes in species richness and community

724 productivity during succession on the Loess Plateau(China). *Pol J Ecol* 58:  
725 501-510.

726 Wei X, Huang L, Xiang Y, Shao M, Zhang X, Gale W (2014) The dynamics of soil  
727 OC and N after conversion of forest to cropland. *Agr Forest Meteorol* 194:  
728 188-196. doi: <https://doi.org/10.1016/j.agrformet.2014.04.008>.

729 Wei XR, Shao MG, Gale WJ, Zhang XC, Li LH (2013) Dynamics of  
730 aggregate-associated organic carbon following conversion of forest to  
731 cropland. *Soil Biol Biochem* 57: 876-883. doi: 10.1016/j.soilbio.2012.10.020.

732 Yamamoto S, Endo T (2014) Soils on the Loess Plateau. In: A Tsunekawa, G Liu, N  
733 Yamanaka, S Du (eds) *Restoration and Development of the Degraded Loess*  
734 *Plateau, China*. Springer Japan, Tokyo.

735 Yamanaka N, Hou Q-C, Du S (2014) Vegetation of the Loess Plateau. In: A  
736 Tsunekawa, G Liu, N Yamanaka, S Du (eds) *Restoration and Development of*  
737 *the Degraded Loess Plateau, China*. Springer Japan, Tokyo.

738 Zhang J, Taniguchi T, Tateno R, Xu M, Du S, Liu G-B, Yamanaka N (2013)  
739 Ectomycorrhizal fungal communities of *Quercus liaotungensis* along local  
740 slopes in the temperate oak forests on the Loess Plateau, China. *Ecol Res* 28:  
741 297-305. doi: 10.1007/s11284-012-1017-6.

742 Zhang KR, Dang HS, Zhang QF, Cheng XL (2015) Soil carbon dynamics following  
743 land-use change varied with temperature and precipitation gradients: evidence  
744 from stable isotopes. *Global Change Biol* 21: 2762-2772. doi:  
745 10.1111/gcb.12886.

746 Zhao Y-G, Liu X-F, Wang Z-L, Zhao S-W (2015) Soil organic carbon fractions and  
747 sequestration across a 150-yr secondary forest chronosequence on the Loess  
748 Plateau, China. CATENA 133: 303-308. doi:  
749 <https://doi.org/10.1016/j.catena.2015.05.028>.

750 Zhou P, Wen A, Zhang X, He X (2013) Soil conservation and sustainable  
751 eco-environment in the Loess Plateau of China. Environ Earth Sci 68: 633-639.  
752 doi: 10.1007/s12665-012-1766-0.

753 Zhou WJ, An ZS, Lin BH, Xiao JL, Zhang JZ, Xie J, Zhou MF, Porter SC, Head MJ,  
754 Donahue DJ (1992) Chronology of the baxie loess profile and the history of  
755 monsoon climates in China between 17000 and 6000 years BP. Radiocarbon  
756 34: 818-825.

757 Zhu G, Shangguan Z, Deng L (2021) Dynamics of water-stable aggregates associated  
758 organic carbon assessed from delta C-13 changes following temperate natural  
759 forest development in China. Soil Till Res 205: 104782. doi:  
760 <https://doi.org/10.1016/j.still.2020.104782>.

761 Zhu YZ, Cheng P, Yu SY, Yu HG, Kang ZH, Yang YC, Jull AJT, Lange T, Zhou WJ  
762 (2010) Establishing a firm chronological framework for neolithic and early  
763 dynastic archaeology in the shangluo area, central China. Radiocarbon 52:  
764 466-478.

765 Zou H, Liu G, Wang H (2001) The vegetation development in North Ziwulin forest  
766 region in last fifty years. Acta Botanica Boreali-Occidentalia Sinica 22: 1-8.  
767

768  
769  
770

Table 1 The characters of soil at 0-10cm and 20-20cm depth of the three land-use systems (AF, AR and NQ) in semiarid Loess Plateau of China<sup>a</sup>

land-use system	depth	NQ	Paired-NQ <sup>b</sup>	AR	Paired-AR	AF	Paired-AF
SOC (%)	0-10cm	3.32±0.42	3.38±0.23	1.71±0.19	1.81±0.15	0.99±0.09	1.07±0.03
	10-20cm	1.27±0.11	1.19±0.13	0.87±0.12	0.92±0.08	0.81±0.02	0.79±0.05
Total N (%)	0-10cm	0.26±0.02	0.23±0.03	0.18±0.01	0.18±0.03	0.10±0.01	0.11±0.01
	10-20cm	0.12±0.02	0.11±0.01	0.09±0.01	0.11±0.02	0.09±0.02	0.08±0.01
Total P (g kg <sup>-1</sup> )	0-10cm	0.62±0.05	0.63±0.03	0.69±0.07	0.66±0.02	0.59±0.05	0.61±0.02
	10-20cm	0.66±0.01	0.62±0.04	0.67±0.05	0.65±0.03	0.61±0.01	0.62±0.02
Fast K (mg kg <sup>-1</sup> )	0-10cm	142.88±7.76	137.53±6.33	190.13±10.67	197.19±9.86	76.20±7.10	82.37±5.99
	10-20cm	145.91±9.37	141.21±8.92	186.78±11.56	192.18±10.45	73.19±8.17	80.15±
pH	0-10cm	8.23±0.11	8.19±0.05	8.45±0.04	8.43±0.02	8.48±0.12	8.50±0.09
	10-20cm	8.09±0.10	8.12±0.02	8.36±0.09	8.30±0.06	8.43±0.10	8.39±0.11
Bulk Density (g mm <sup>-3</sup> )	0-10cm	0.99±0.04	1.02±0.05	1.16±0.04	1.13±0.05	1.30±0.03	1.28±0.02
	10-20cm	1.18±0.01	1.16±0.03	1.17±0.02	1.15±0.02	1.25±0.02	1.27±0.04

771 a. AF: abandoned farmland; AR: black locust plantation; QF: natural oak forest.

772 b. The distance between paired sites (NQ & paired NQ; AR & paired AR; AF & paired AF) in same land-use system is over 3km for comparing both of soil characters  
773 in the semiarid region.

774 Table 2 The information on study sites of published studies <sup>a</sup>

Conversion type	Land-use system	Distance <sup>b</sup>	Reference
Deforestation	Natural forest; Cropland	>3km	Wei et al. (2013)
Natural restoration	Farmland; Grass land; Natural forest	~5km	Deng et al. (2013)
Deforestation	Natural forest; Cropland	>3km	Wei et al. (2014)
Natural & artificial restoration	Natural forest; Plantation	>1.5km	Song et al. (2016)
Natural restoration	Farmland; Grass land; Natural forest	>3km	Deng et al. (2016)
Natural restoration	Grass land; Natural forest	>5km	Zhu et al. (2021)

775 a. The published studies were carried out by using “space-for-time substitution” method in  
776 the same study area with current study.

777 b. Distance means the distance among different land-use systems

778 Figure captions

779 Fig 1 Soil organic carbon (SOC) stock (a) and soil organic carbon contents (b) at each  
780 depth (0-10cm, 10-20cm, 20-30cm, 30-50cm and 50-100cm) of the three different  
781 land-use systems. Error bars represent the standard error of the mean. Significant  
782 differences are indicated by the different letter ( $p < 0.05$ ); AF: abandoned farmland;  
783 AR: artificial afforestation (plantation of *Robinia pseudoacacia* L); NQ: natural  
784 afforestation (natural forest - *Quercus liaotungensis* Koidz).

785

786 Fig 2 The different aggregate size OC stocks (a) and size class distributions (b) in the  
787 three land-use systems. Macroaggregates were  $>0.25$  mm; microaggregates were  
788 between 0.25 and 0.053 mm; and silt & clay were  $<0.053$  mm. Error bars represent the  
789 standard error of the mean. Significant differences are indicated by different letter ( $p$   
790  $< 0.05$ ); AF: abandoned farmland; AR: artificial afforestation (plantation of *Robinia*  
791 *pseudoacacia* L); NQ: natural afforestation (natural forest - *Quercus liaotungensis*  
792 Koidz).

793

794 Fig 3 The C:N and C:P of different soil aggregate size classes in the three land-use  
795 systems. Macroaggregates were  $>0.25$  mm; microaggregates were between 0.25 and  
796 0.053 mm; and silt & clay were  $<0.053$  mm. Error bars represent the standard error of  
797 the mean. Significant differences are indicated by the different letter ( $p < 0.05$ ); AF:  
798 abandoned farmland; AR: artificial afforestation (plantation of *Robinia pseudoacacia*  
799 L); NQ: natural afforestation (natural forest - *Quercus liaotungensis* Koidz).

800 Fig 4 SOC decomposition rate constants ( $k_1$ ) and new SOC input rate ( $\text{kg m}^{-2} \text{yr}^{-1}$ )  
801 calculated with a  $^{13}\text{C}$  model under (a) artificial and (b) natural afforestation. Error bars  
802 represent the standard error of the mean. Significant differences are indicated by the  
803 asterisk symbol ( $*p < 0.05$ ).

804

805 Fig 5 SOC decomposition rate constants ( $k_2$ ) calculated with a  $^{14}\text{C}$  model for different  
806 land use types. Error bars represent the standard error of the mean. Significant  
807 differences are indicated by different letters ( $p < 0.05$ ). AF: abandoned farmland; AR:  
808 artificial afforestation (plantation of *Robinia pseudoacacia* L); NQ: natural  
809 afforestation (natural forest - *Quercus liaotungensis* Koidz).

810

811 Fig 6 The mean annual soil  $\text{CO}_2$  emission over 4 years in the three land-use systems.  
812 Error bars represent the standard error of the mean. Significant differences are  
813 indicated by the different letter ( $p < 0.05$ ); AR: artificial afforestation (plantation of  
814 *Robinia pseudoacacia* L); NQ: natural afforestation (natural forest - *Quercus*  
815 *liaotungensis* Koidz).

816

817 Fig 7 Changes in SOC stocks in macroaggregates and microaggregates with  
818 afforestation under (a-b) artificial and (c-d) natural restoration. Macroaggregates  
819 were  $>0.25$  mm; microaggregates were between 0.25 and 0.053 mm; and silt & clay  
820 were  $<0.053$  mm. Error bars represent the standard error of the mean. Significant  
821 differences are indicated by the asterisk symbol ( $*p < 0.05$ ); ns: no significant. AF:

822 abandoned farmland; AR: artificial afforestation (plantation of *Robinia pseudoacacia*

823 L); NQ: natural afforestation (natural forest - *Quercus liaotungensis* Koidz).

824

825

## Conflict of Interest

826 ● All authors declare no conflict of interest.

827

# Figures

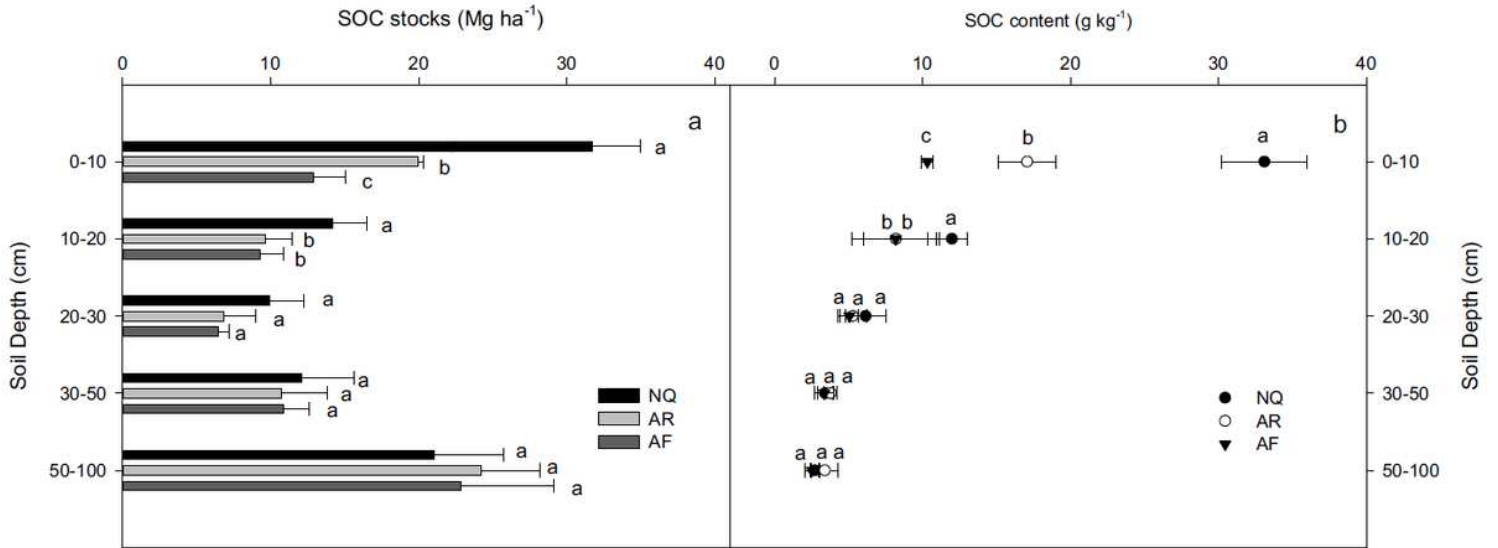


**Figure 1**

Soil organic carbon (SOC) stock (a) and soil organic carbon contents (b) at each depth (0-10cm, 10-20cm, 20-30cm, 30-50cm and 50-100cm) of the three different land-use systems. Error bars represent the standard error of the mean. Significant differences are indicated by the different letter (p < 0.05); AF: abandoned farmland; AR: artificial afforestation (plantation of *Robinia pseudoacacia* L); NQ: natural afforestation (natural forest - *Quercus liaotungensis* Koidz).

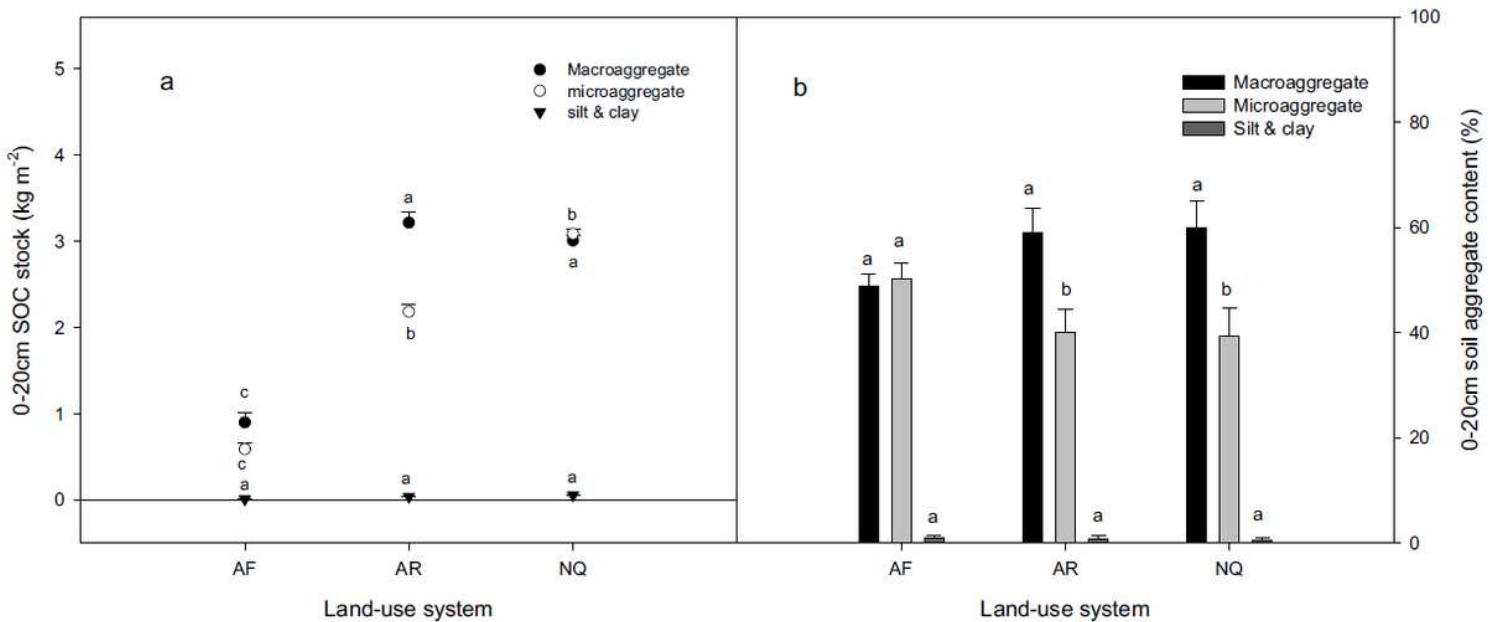


**Figure 2**

The different aggregate size OC stocks (a) and size class distributions (b) in the three land-use systems. Macroaggregates were >0.25 mm; microaggregates were between 0.25 and 0.053 mm; and silt & clay were <0.053 mm. Error bars represent the standard error of the mean. Significant differences are indicated by different letter ( $p < 0.05$ ); AF: abandoned farmland; AR: artificial afforestation (plantation of *Robinia pseudoacacia* L); NQ: natural afforestation (natural forest - *Quercus liaotungensis* Koidz).

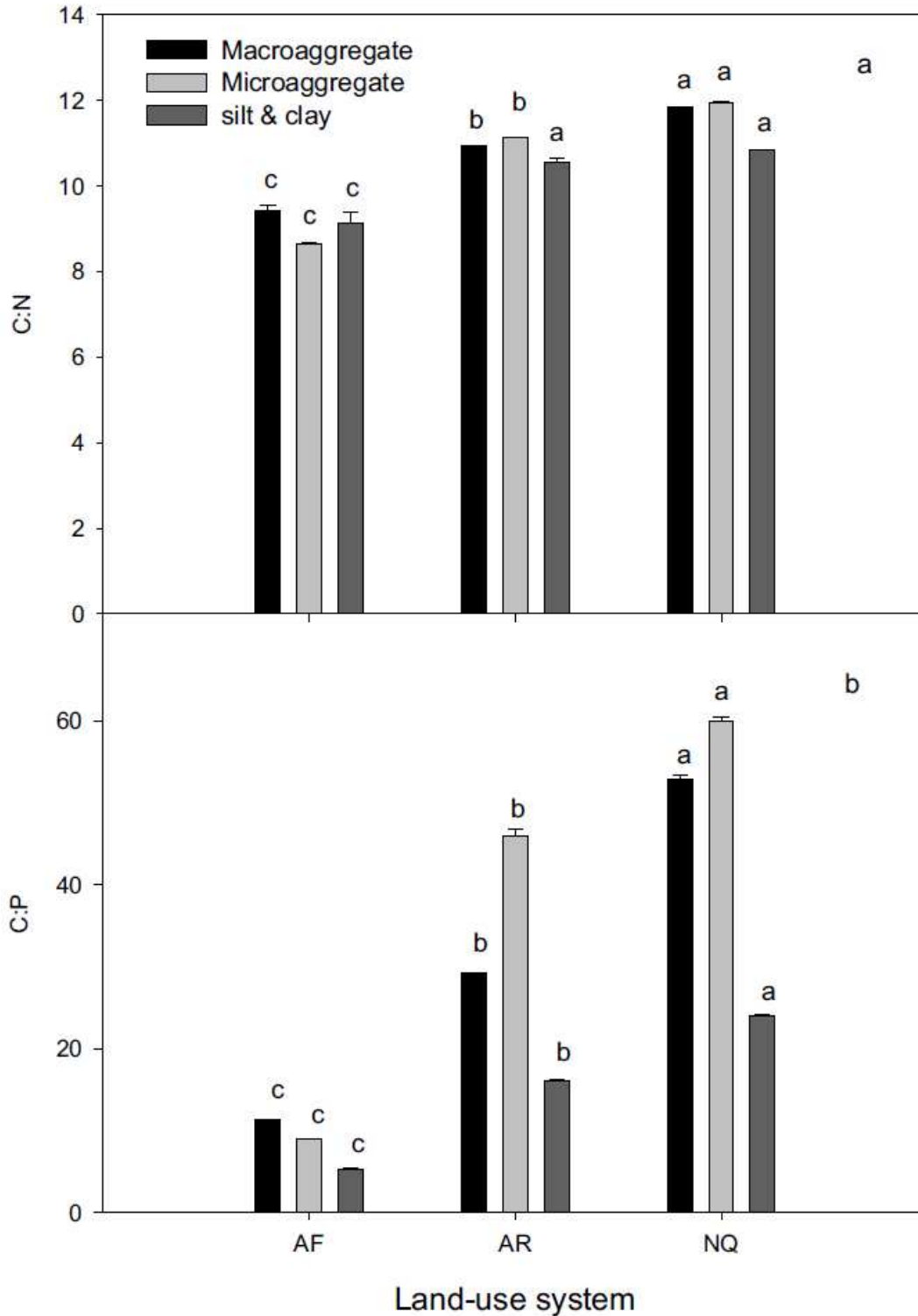


Figure 3

The C:N and C:P of different soil aggregate size classes in the three land-use systems. Macroaggregates were >0.25 mm; microaggregates were between 0.25 and 0.053 mm; and silt & clay were <0.053 mm. Error bars represent the standard error of the mean. Significant differences are indicated by the different letter (p < 0.05); AF: abandoned farmland; AR: artificial afforestation (plantation of *Robinia pseudoacacia* L); NQ: natural afforestation (natural forest - *Quercus liaotungensis* Koidz).

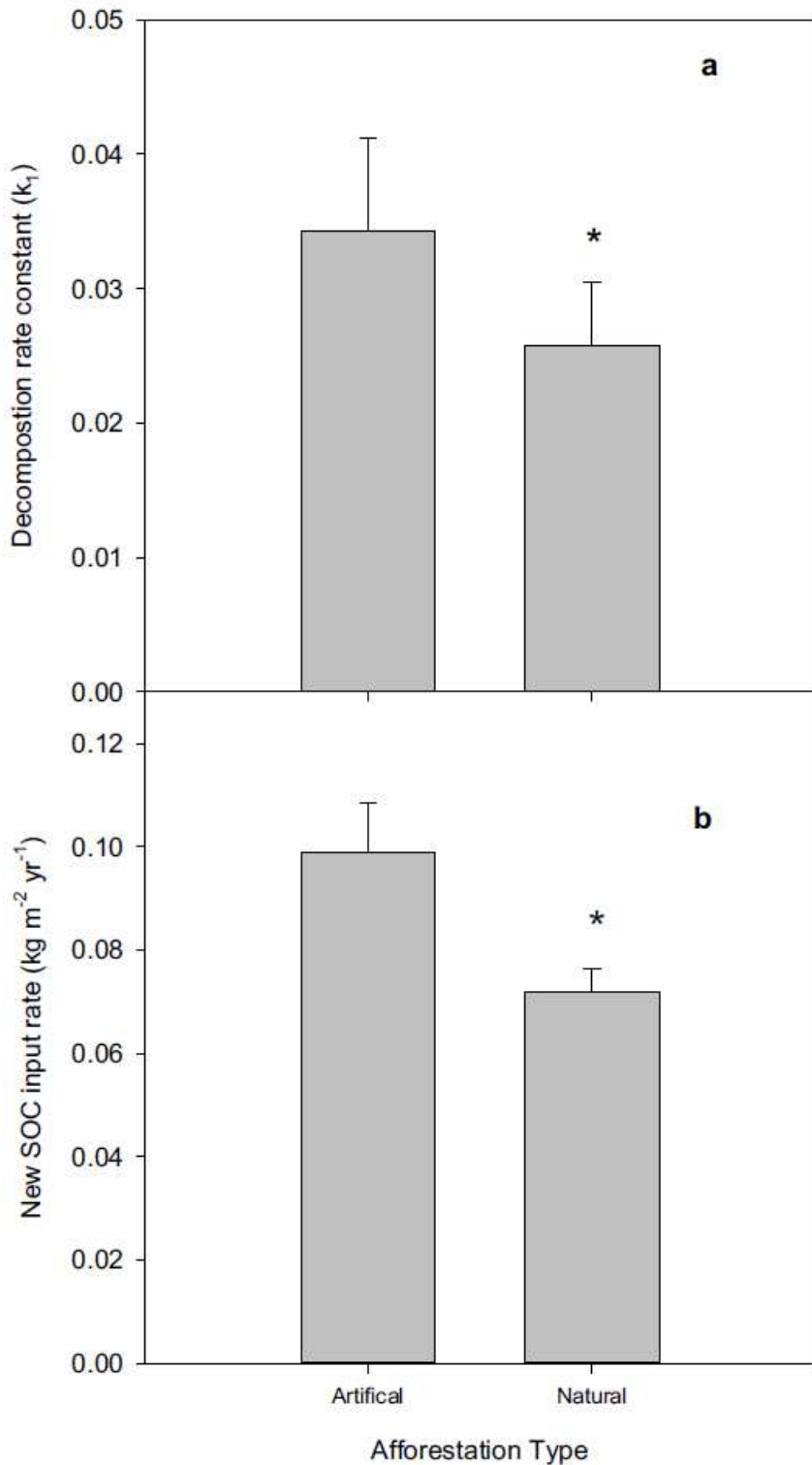
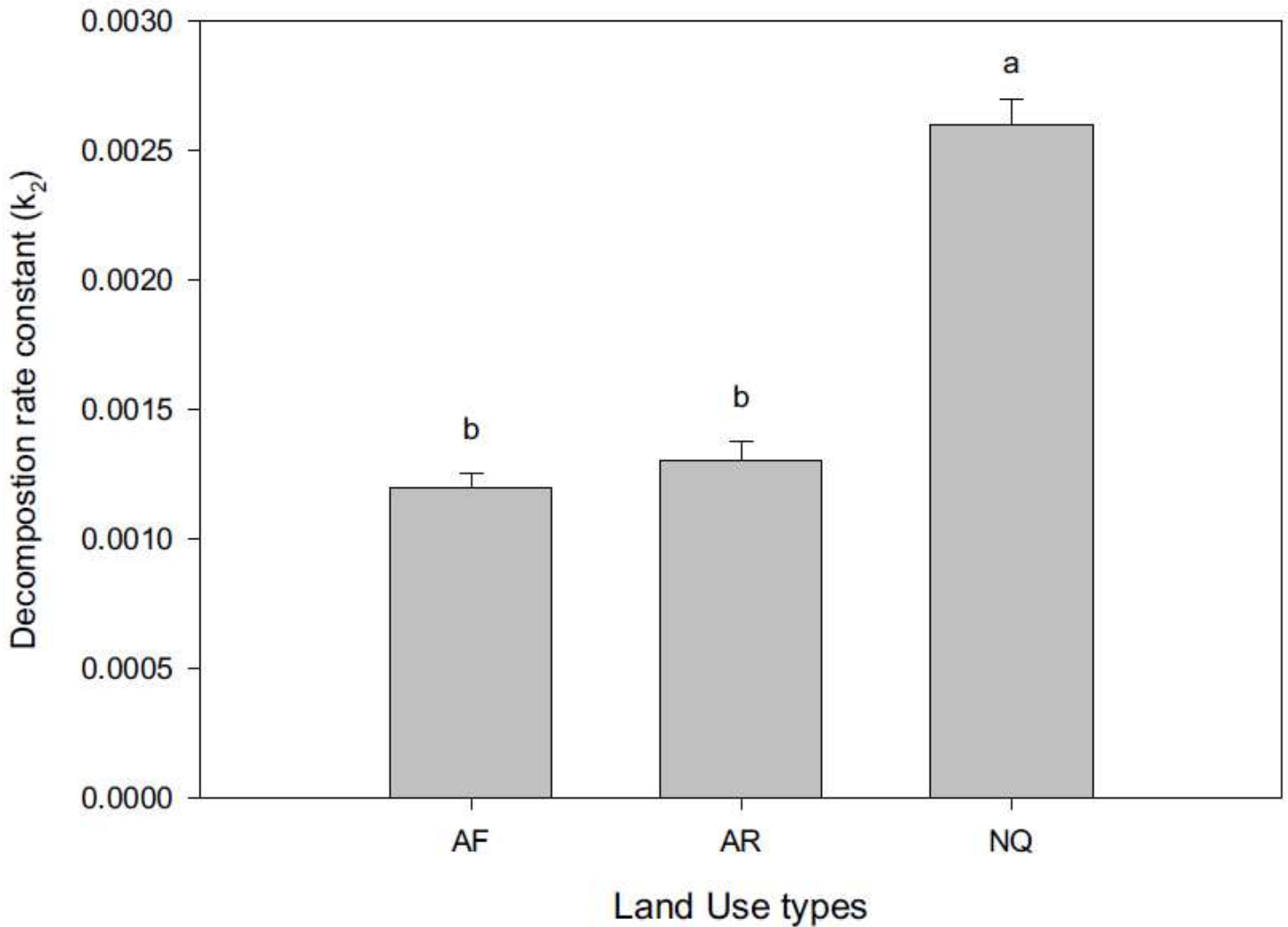


Figure 4

SOC decomposition rate constants ( $k_1$ ) and new SOC input rate ( $\text{kg m}^{-2} \text{yr}^{-1}$ ) calculated with a  $^{13}\text{C}$  model under (a) artificial and (b) natural afforestation. Error bars represent the standard error of the mean. Significant differences are indicated by the asterisk symbol ( $*p < 0.05$ ).



**Figure 5**

SOC decomposition rate constants ( $k_2$ ) calculated with a  $^{14}\text{C}$  model for different land use types. Error bars represent the standard error of the mean. Significant differences are indicated by different letters ( $p < 0.05$ ). AF: abandoned farmland; AR: artificial afforestation (plantation of *Robinia pseudoacacia* L); NQ: natural afforestation (natural forest - *Quercus liaotungensis* Koidz).

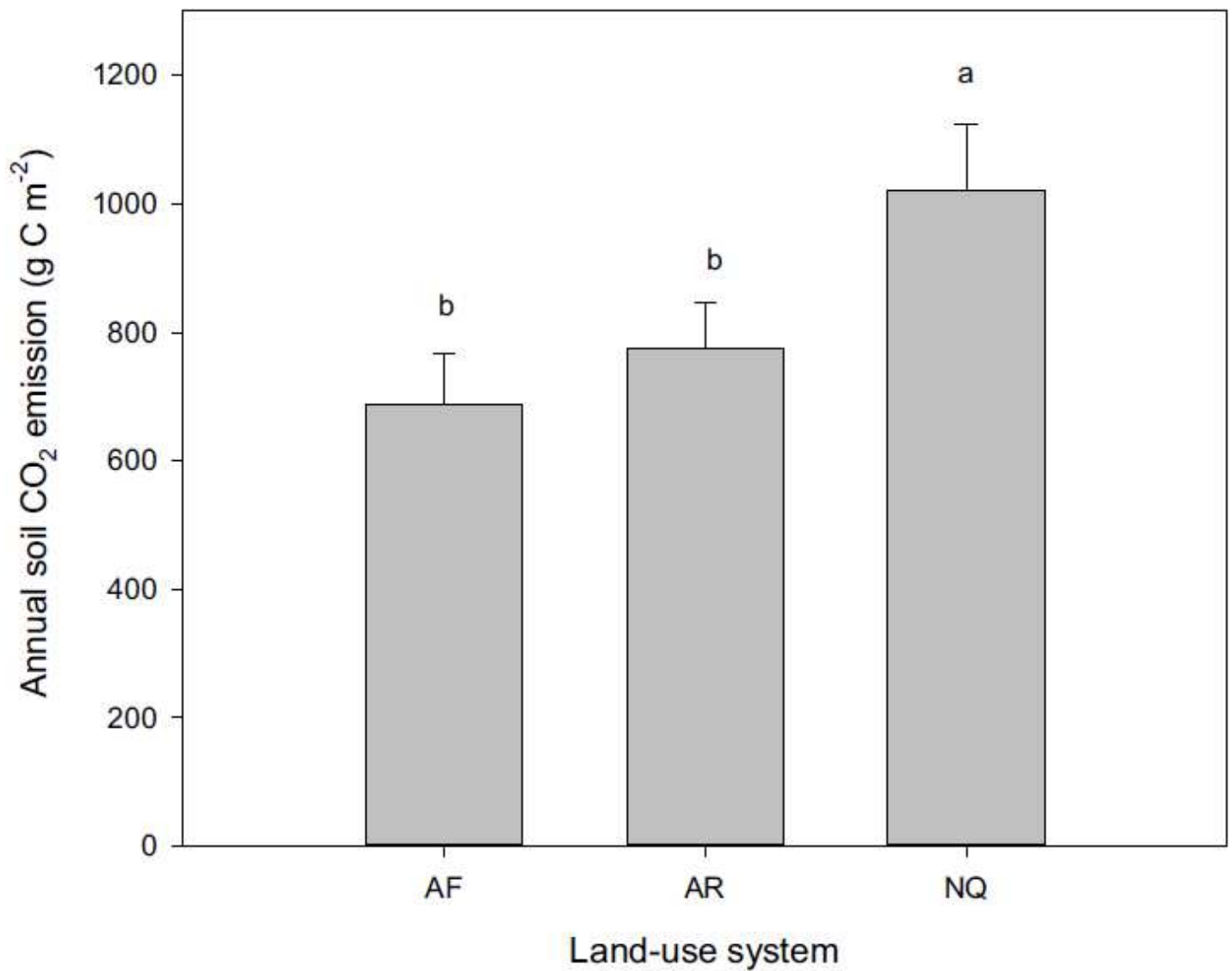


**Figure 6**

The mean annual soil CO<sub>2</sub> emission over 4 years in the three land-use systems. Error bars represent the standard error of the mean. Significant differences are indicated by the different letter ( $p < 0.05$ ); AR: artificial afforestation (plantation of *Robinia pseudoacacia* L); NQ: natural afforestation (natural forest - *Quercus liaotungensis* Koidz).

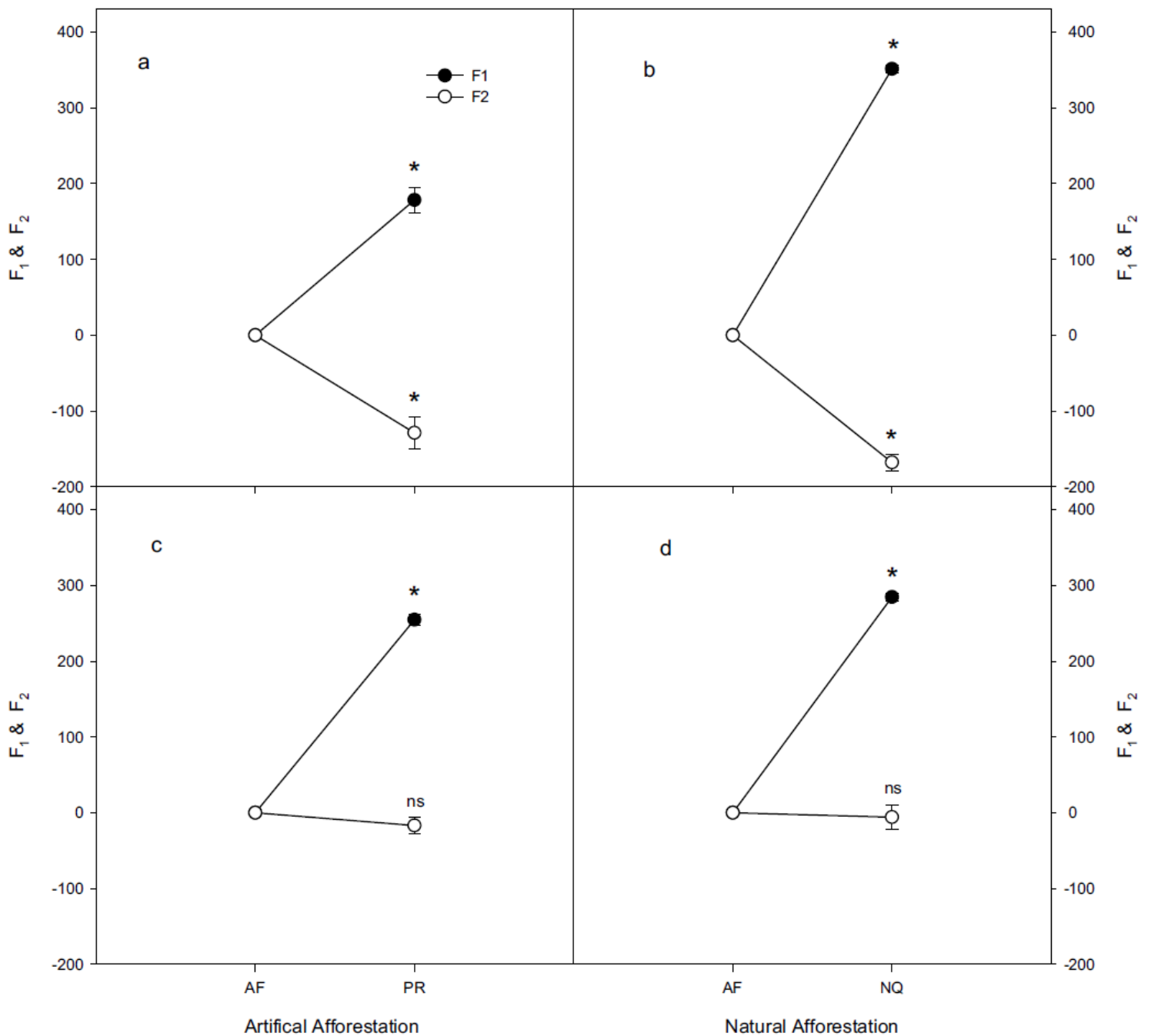


**Figure 7**

Changes in SOC stocks in macroaggregates and microaggregates with afforestation under (a-b) artificial and (c-d) natural restoration. Macroaggregates were >0.25 mm; microaggregates were between 0.25 and 0.053 mm; and silt & clay were <0.053 mm. Error bars represent the standard error of the mean. Significant differences are indicated by the asterisk symbol (\* $p < 0.05$ ); ns: no significant. AF: abandoned farmland; AR: artificial afforestation (plantation of *Robinia pseudoacacia* L); NQ: natural afforestation (natural forest - *Quercus liaotungensis* Koidz).